DPIV INVESTIGATION OF A TURBULENT BOUNDARY LAYER MANIPULATED BY TRANSVERSAL WALL OSCILLATIONS

G. M. DI CICCA†, G. IUSO†, M. ONORATO†, P. G. SPAZZINI‡
†DIASP, Politecnico di Torino
C.so Duca degli Abruzzi, 24 - I 10129 Torino (ITALY) &
‡IMGC - CNR c/o DIASP, Politecnico di Torino

Keywords: *DPIV, Wall-Oscillations, Turbulent Boundary Layer*

Abstract

The effects of transversal wall oscillations on a turbulent boundary layer developing on a flat plate have been studied by means of Digital Particle Image Velocimetry (DPIV).

Results are presented for the optimum oscillation period of 100 viscous time units and for an oscillation amplitude of 320 viscous units. Turbulent velocity fluctuations are considerably reduced by the wall oscillations.

Comparisons between the canonical and forced flow have been performed in an attempt at observing the physical mechanisms by which the wall oscillation influences the near wall organized motions.

1 Introduction

A turbulent boundary layer is characterized by dominant coherent motions (trains of quasi-longitudinal vortical structures and quasi-streamwise velocity streaks [16, 15]), spanning the region up to approximately $y^+ = 100$. It has also long been recognised that vortical motions cause the velocity streaks by advecting the mean momentum gradient (see e.g. [2]) and that several vortical structures are associated with each streak (see e.g. [9]), but the physical process leading to the creation of new vortical structures is not yet understood to a satisfactory degree.

The aim of the present paper is focused on a better understanding of the physics of the near wall turbulence by studying its response to external perturbation. The present work deals with a flat plate turbulent boundary layer forced by spanwise oscillations of the wall.

This kind of flow control is not a new research subject; indeed it is well known that appropriate 3-dimensional disturbances introduced into the flow produce friction drag and turbulence reductions. The cause of these reductions is not yet completely understood.

Jung *et al.* [12] conducted a DNS study of a turbulent channel flow subject either to an oscillatory spanwise cross-flow or to spanwise oscillatory motions of one of the channel walls. Their results indicate a 40% reduction in friction drag when the non-dimensional period of oscillation T^+ was set to 100. The oscillations also gave rise to a 40% reduction in the streamwise component of the Reynolds stress, with no significant increase in the spanwise component. These friction drag and turbulence reduction results were experimentally confirmed by Laadhari *et al.* [14] for a boundary layer flow at $Re_\vartheta = 950$. In this paper it was conjectured that the continuous shifting of the longitudinal vortices to different positions relative to the wall velocity streaks weakens the intensity of the streaks, by injecting

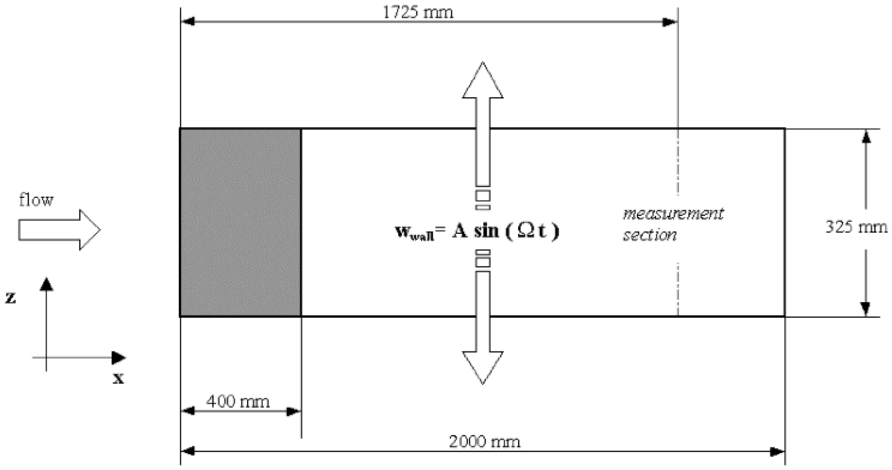

Fig. 1 Scheme of the oscillating flat plate. Dimensions in millimeters.

high speed fluid into low speed zones and low speed fluid into high speed regions. The effect of the wall-oscillation amplitude on the total energy balance was investigated by Baron & Quadrio [1] using DNS. For an oscillation period of $T^+ = 100$ they found 10% of net energy saving with a spanwise wall velocity oscillation amplitude of $Q_x/8h$, where Q_x is the streamwise flow rate per unit width for the unperturbed flow and h is the channel half height. An experimental investigation into changes in the turbulent boundary layer structure with spanwise wall oscillations was carried out by Choi *et al.* [5] and Choi [4]. In agreement with previously mentioned DNS and laboratory experiments a reduction of 45% in the skin friction coefficient was measured with wall oscillations. Choi *et al.* [5] and Choi [4] related the mechanism of drag reduction by spanwise wall oscillations to the spanwise vorticity generated by the periodic Stokes layer over the oscillating wall. Dhanak & Si [7] could demonstrate numerically that the interaction between evolving, axially stretched, streamwise vortices and a Stokes layer on the oscillating surface beneath them leads to reductions in skin friction.

2 Experimental Set-Up

Experiments were carried out in the Hydra water tunnel. This facility is a closed loop, open surface channel with 350mm x 500mm x 1800mm test section. Measurements were taken on a horizontal flat plate (see sketch in Fig. 1). The sinusoidal oscillation of the plate span the whole test section from wall to wall, and was produced by a crank-shaft system with an operating frequency in the range from 0 to 5 Hz. The results presented here refer to a wall oscillation frequency of 2.67 Hz, corresponding to a period of 100 viscous units, $T^+ = 100$. The peak-to-peak amplitude of the moving wall was 2 cm, corresponding to $\Delta z^+ = 324$. Viscous units are here referred to the case of absence of wall oscillation.

The water of the tunnel was seeded with spherical solid particles, 2μm nominal diameter. A Nd-YAG laser source with 200mJ of energy per pulse and a duration of 8ns provided double-pulsed light sheets (approximately 0.5 mm thick) with a repetition rate of 10 Hz. Images were recorded using a 1008 x 1012 pixels CCD videocamera (Kodak Megaplus ES 1.0).

The standard turbulent boundary layer flow was characterised by $Re_\vartheta = 1160$, $H = 1.32$, $u_\tau/U_e = 0.044$, $\delta = 43$ mm and an external free-stream turbulence of 1.2%.

PIV measurements were taken in a plane (x,z) parallel to the wall and in a streamwise plane (x,y) normal to the wall; x is the streamwise coordinate. The (x,z) images were situated in the buffer layer at a distance of 20 viscous units from the wall, $y^+ = 20$; the images in the plane (x,y) span the buffer layer and about the whole logarithmic region, as y^+ ranges from 0 to 310.

The local particle-image displacement was determined by using a cross correlation based algorithm, structured as an iterative multigrid method [17]. The final interrogation window size was 32x32 pixels and an overlapping of 50% was used.

After being computed by interrogating every image-couple, vector fields were validated by applying standard post processing procedures [8]. Each vector represents a locally filtered value of the velocity in a physical dimension (Δx, Δy, Δz) corresponding respectively to ($\Delta x^+ = 17.8$, $\Delta y^+ = 8.1$, $\Delta z^+ = 17.8$) in the plane (x,z) and to ($\Delta x^+ = 10.4$, $\Delta y^+ = 10.4$, $\Delta z^+ = 8.1$) in the plane (x,y). The spatial resolution in the (x,z) plane is then equal to about 10 Kolmogorov lengthscales, while in the (x,y) plane, for $y^+ > 100$, it ranges (in the wall normal direction) from 3.1 to 4.1 Kolmogorov lengthscales.

Statistical analysis was performed by averaging over 600 PIV images in both planes (x,z) and (x,y).

3 Results and Comments

Mean velocity profiles are first displayed in the log-law plot of Fig. 2; the manipulated velocity profiles were normalized against the friction velocities of both the canonical and forced cases. Wall-shear stress was evaluated by means of the near-wall slope of the mean velocity profile and was confirmed by the fact that the mean velocity U in the first measurement points in the viscous sublayer, when normalised with respect to the estimated value of the friction velocity, satisfies the expected relation $U^+ = y^+$ [5]. The marked upward shifting of the logarithmic velocity profile for the forced flow, when actual inner-scaling (i.e. the one performed with the inner variables corresponding to the case being discussed) is applied, confirms that the skin-friction drag is reduced by spanwise wall oscillation. This indication is typical of most drag reducing flows and suggests the thickening of the viscous sublayer. When quantities are normalized with respect to the friction velocity of the standard boundary layer, a reduction of the mean velocity is observed throughout the region $y^+ < 30$. Farther from the wall the mean velocity is slightly larger in order to conserve momentum.

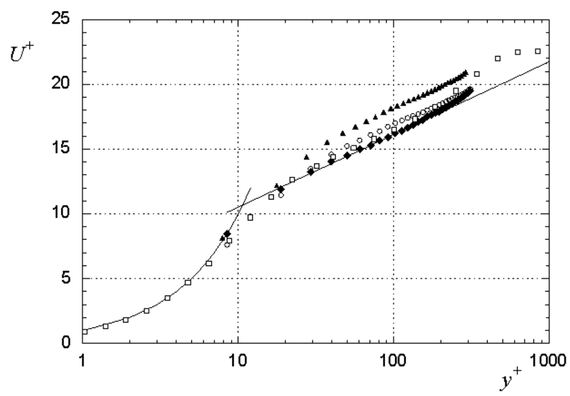

Fig. 2 Log-law plot of mean velocity profiles. Solid line: law of the wall; full diamonds: standard boundary layer; empty circles: manipulated boundary layer (u_τ standard boundary layer); full triangles: manipulated boundary layer (actual u_τ); empty squares: LDV data from [6] for standard boundary layer

Velocity fluctuation results are compared in Fig. 3, where considerably large reductions in both components of the velocity variance, longitudinal u'^2 and wall normal v'^2, are shown within the inner region. The maximum u'^2 and v'^2 reductions, located in the buffer region, are of the order of 30% and 40% respectively.

The distribution of Reynolds shear stress is displayed in Fig. 4 as a function of the distance from the wall, for the natural and the forced flow. Reynolds stress are scaled with the friction velocity referred to the natural case. It is clearly visible a sensible reduction all over the investigated region of the boundary layer. Particularly in the inner region a reduction by up to 50% is obtained.

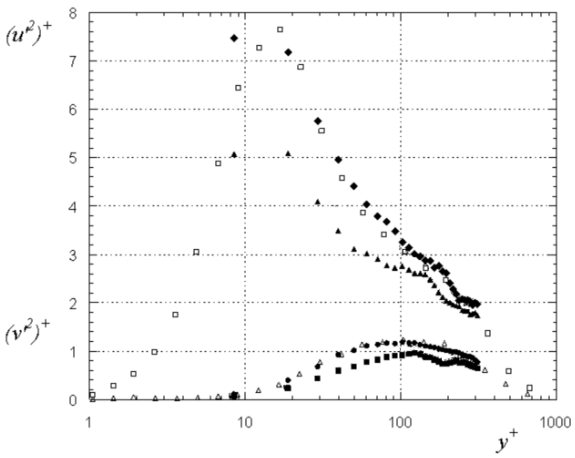

Fig. 3 Profiles of velocity component variance. Full diamonds: $(u'^2)^+$ standard boundary layer; full triangles: $(u'^2)^+$ manipulated boundary layer (u_τ standard boundary layer); full circles: $(v'^2)^+$ standard boundary layer; full squares: $(v'^2)^+$ manipulated boundary layer (u_τ standard boundary layer); empty symbols: LDV data from [6] for standard boundary layer

In order to observe the overall structure of the flow, Fig. 5 displays the double spatial correlation function, R_{uu}, for the streamwise fluctuating velocity at a distance of $y^+ = 20$ from the wall. A marked increase in the integral lateral scale produced by the wall oscillation clearly appears. An explanation of this behaviour could be related to an increasing of the low speed streaks mean spacing. A result pointing in the same direction is reported in [5], where infrared images show that several low speed streaks coalesce into a single streak as the wall oscillates, leading the mean streak spacing to increase by about 45%.

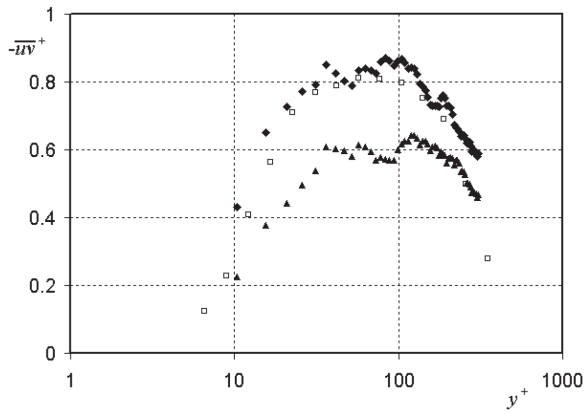

Fig. 4 Reynolds shear stress profiles. Diamonds: standard boundary layer; triangles: manipulated boundary layer; empty symbols: LDV data from [6] for standard boundary layer

In order to gather information about the streaks' strength it is helpful to observe in Fig. 6 the probability density functions of the normal fluctuating vorticity ω_y, in planes $y^+ = 20$. In Fig. 6, ω_y is normalized with respect to the root mean square value of the natural flow vorticity, ω'_y, at $y^+ = 20$. Comparison between the standard and the forced boundary layers shows that the PDF tails assume considerably lower values for the manipulated flow. This behaviour of the PDFs may be interpreted as the consequence of the weakening action of the wall oscillation on the velocity streaks. Jimenez & Pinelli [10] showed by a numerical experiment that, by filtering the high values of ω_y flanking the low speed streaks, a turbulent flow can be brought to decay back to a laminar state. The present result experimentally confirms the association between the weakening of the velocity str eaks, and therefore their stabilization [18], and the reductions in near wall turbulence and skin friction.

The creation of internal inclined shear layer structures has been historically considered an important feature of the near-wall flow

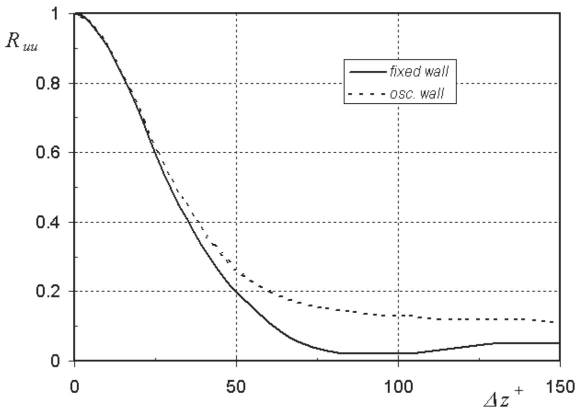

Fig. 5 Spanwise correlation functions R_{uu}. $y^+ = 20$. Solid line: natural boundary layer; broken line: manipulated boundary layer

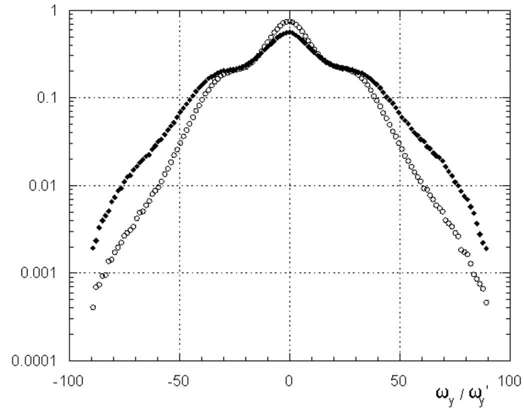

Fig. 6 Probability density functions of ω_y. $y^+ = 20$. Full diamond: natural boundary layer; empty circle: manipulated boundary layer

field (see e.g. [11]). In the present work, internal shear layer motions were detected by applying the VISA technique [13], which is the spatial counterpart of VITA technique [3], widely used in hot wire and LDV measurements. It is of interest to observe the effect of the manipulation on the spatial frequency of occurrence of internal shear layer events n and on their structure. In Fig. 7 the non-dimensional frequency of the occurring events n^+, at $y^+ = 20$, as a function of the short integration length L^+ and of the threshold constant k is reported. The short integration length is scaled with respect to the standard boundary layer inner variables. The curves plotted in Fig. 7 show that, whatever the short integration length and the threshold constant, the number of internal shear layer events is reduced by the wall oscillation. Reduction in bursting frequency was also observed by Choi *et al.* [5] and by Baron & Quadrio [1].

Finally, it has been shown by Laadhari *et al.* [14] that the spanwise oscillation affects also the fine structure of the turbulence. This is confirmed by the present PIV results shown in Fig. 8, where the distribution of non dimensional Taylor's microscales is given by ${\lambda_{11}}^{(i)+} = u_\tau/\nu\sqrt{\overline{u^2}/\overline{(\partial u/\partial x_i)^2}}$ (here $x_1 = x$ and $x_2 = y$). It can be seen that both dissipation length scales are reduced with a greater reduction in ${\lambda_{11}}^{(1)+}$ by the wall oscillation for $y^+ < 40$.

4 Conclusions

Longitudinal and wall normal turbulent velocity fluctuations as well as Reynolds shear stresses are considerably reduced by wall oscillations; the amount of the reduction is comparable to numerical and experimental results from the literature.

The observed thickening of the viscous wall sublayer for the forced flow, evidenced by the upward shifting of the logarithmic velocity profile, reflects a clear reorganization of the near wall turbulent structures, involving presumably an increase in the small eddies scale and a displacement of the turbulent events outwards from the wall.

The spanwise integral length scale is increased by the manipulation; this may reflect an increase of the low speed streaks spacing, presumably due to the enhanced mixing near the wall caused by the presence of oscillating Stokes layers. These transversally oscillating layers, besides being the cause of the mean ve-

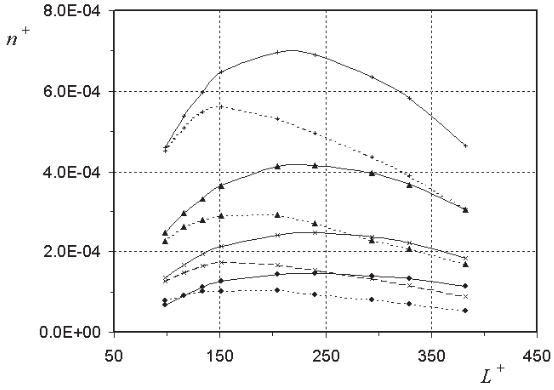

Fig. 7 Frequency of the occurring VISA events, n^+. $y^+ = 20$. Solid lines: natural boundary layer; broken lines: manipulated boundary layer. Plus: $k = 0.6$; full triangle: $k = 0.8$; cross: $k = 1.0$; full circle: $k = 1.2$

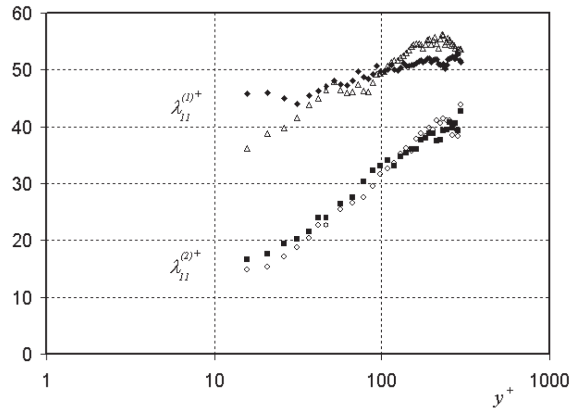

Fig. 8 Taylor's microscales. Diamonds and squares: natural boundary layer; empty circles and triangles: manipulated boundary layer

locity gradient reduction at the wall (according to Choi *et al.* [5]), may induce continuous shifting of the near wall longitudinal vortices relative to the velocity streaks, thus weakening the low speed streaks. This is evidenced by the reduction in the high value range of the wall normal vorticity in the manipulated case and confirms the association between the weakening of the velocity structures with the reduction of the near wall turbulence activity.

In the manipulated flow the occurrence of less internal shear layer events (VISA events) also proves the weakening of the velocity streaks.

The main results in this investigation are consistent with the scenario in which the oscillating transversal layers weaken and stabilize the wall velocity streaky structures, causing the attenuation of the regeneration mechanisms of the longitudinal streamwise vortices (see [18]) and then the reduction of the wall turbulence activities.

Acknowledgments

This work was supported by grants from the CNR and MURST. The Authors wish to thank Mr. Grivet, Mr. Masili and Mr. Savorelli, technical personnel, for their help in building and setting up the experimental devices.

References

[1] A. Baron and M. Quadrio. Turbulent Drag Reduction by Spanwise Wall Oscillations. *Appl. Sci. Res.*, 55:311–326, 1996.

[2] R. Blackwelder and H. Eckelmann. Streamwise Vortices Associated with the Bursting Phenomenon . *Journal of Fluid Mechanics*, 94:577–594, 1979.

[3] R. Blackwelder and R. E. Kaplan. On the Wall Structure of Turbulent Boundary Layers. *Journal of Fluid Mechanics*, 76:89–112, 1978.

[4] K. S. Choi. European Drag Reduction - Research Recent Developments and Current Status. *Fluid Dynamics Research*, 26(5):325–335, 2000.

[5] K. S. Choi, J. R. DeBisschop, and B. R. Clayton. Turbulent Boundary Layer Control by Means of Spanwise Wall Oscillations. *AIAA Journal*, 36(7):1157–1163, 1998.

[6] D. B. De Graaf and J. K. Eaton. Reynolds-Number Scaling of the Flat-Plate Turbulent Boundary Layer. *Journal of Fluid Mechanics*, 422:319–346, 2000.

[7] M. B. Dhanak and C. Si. On Reduction of Turbulent Wall Friction through Spanwise Wall Oscillations. *Journal of Fluid Mechanics*, 383:175–195, 1999.

[8] G. M. Di Cicca. Experimental Study of Wall Turbulent Flows and Their Control. PhD thesis, Politecnico di Torino, 2001.

[9] J. Jimenez and P. Moin. The Minimal Flow Unit in Near Wall Turbulence. *Journal of Fluid Mechanics*, 225:221–240, 1991.

[10] J. Jimenez and A. Pinelli. The Autonomous Cycle of Near-Wall Turbulence. *Journal of Fluid Mechanics*, 389:335–359, 1999.

[11] A. V. Johansson, P. H. Alfredsson, and J. Kim. Evolution and Dynamics of Shear Layer Structures in Near-Wall Turbulence. *Journal of Fluid Mechanics*, 224:579–599, 1991.

[12] W. J. Jung, N. Mangiavacchi, and R. Akhavan. Suppression of Turbulence in Wall-Bounded Flows by High-Frequency Spanwise Oscillations. *Physics of Fluids A*, 4(8):1605–1607, 1992.

[13] J. Kim. Turbulence Structures Associated with the Bursting Event. *Physics of Fluids*, 28(1):52–58, 1985.

[14] F. Laadhari, L. Skandaji, and R. Morel. Turbulence Reduction in a Boundary Layer by a Local Spanwise Oscillating Surface. *Physics of Fluids*, 6(10):3218–3220, 1994.

[15] R. L. Panton, editor. *Self-Sustaining Mechanisms of Wall Turbulence*, volume 15 of *Advances in Fluid Mechanics*. Computational Mechanics Publications, Southhampton, UK, 1997.

[16] S. K. Robinson. Coherent Motions in the Turbulent Boundary Layer. *Annual Review of Fluid Mechanics*, 23:601–639, 1991.

[17] F. Scarano and M. L. Riethmuller. Iterative Multigrid Approach in PIV Image Processing with Discrete Window Offset. *Experiments in Fluids*, 26:513–523, 1999.

[18] W. Schoppa and F. Hussain. Coherent Structure Generation in Near-Wall Turbulence. *Journal of Fluid Mechanics*, 453:57–108, 2002.